HHS Public Access

Author manuscript

Neuron. Author manuscript; available in PMC 2017 February 17.

Published in final edited form as:

Neuron. 2016 February 17; 89(4): 734–740. doi:10.1016/j.neuron.2015.12.038.

Pathway-Specific Remodeling of Thalamostriatal Synapses in Parkinsonian Mice

Philip R. L. Parker[1,2], **Arnaud L. Lalive**[2], and **Anatol C. Kreitzer**[1,2,3,*]

[1]Neuroscience Graduate Program, University of California, San Francisco

[2]Gladstone Institutes, San Francisco, CA 94158 USA

[3]Departments of Physiology and Neurology, University of California San Francisco, CA 94158 USA

SUMMARY

Movement suppression in Parkinson's disease (PD) is thought to arise from increased efficacy of the indirect pathway basal ganglia circuit, relative to the direct pathway. However, the underlying pathophysiological mechanisms remain elusive. To examine whether changes in the strength of synaptic inputs to these circuits contribute to this imbalance, we obtained paired whole-cell recordings from striatal direct- and indirect-pathway medium spiny neurons (dMSNs and iMSNs) and optically stimulated inputs from sensorimotor cortex or intralaminar thalamus in brain slices from control and dopamine-depleted mice. We found that dopamine depletion selectively decreased synaptic strength at thalamic inputs to dMSNs, suggesting that thalamus drives asymmetric activation of basal ganglia circuitry underlying parkinsonian motor impairments. Consistent with this hypothesis, *in vivo* chemogenetic and optogenetic inhibition of thalamostriatal terminals reversed motor deficits in dopamine-depleted mice. These results implicate thalamostriatal projections in the pathophysiology of PD and support interventions targeting thalamus as a potential therapeutic strategy.

INTRODUCTION

The underlying pathophysiology of Parkinson's disease (PD) remains poorly understood despite decades of research. The pathological hallmark of PD is a progressive loss of dopamine neurons in the substantia nigra pars compacta, which extensively innervates the dorsal striatum (Ehringer and Hornykiewicz, 1960). Loss of striatal dopamine is proposed to increase efficacy of the indirect pathway basal ganglia circuit (thought to normally suppress movement) and/or decrease efficacy of the direct pathway circuit (thought to normally

*correspondence: akreitzer@gladstone.ucsf.edu.

AUTHOR CONTRIBUTIONS

P.R.L.P. designed and performed all experiments, analyzed data, and wrote the manuscript. A.L.L. designed and performed behavior experiments. A.C.K. designed experiments, wrote the manuscript, and supervised the research.

facilitate movement) (Albin et al., 1989; DeLong, 1990). A number of studies revealed PD-associated intrinsic and synaptic changes in direct and indirect pathway striatal medium spiny neurons (dMSNs and iMSNs) (Day et al., 2006; Fieblinger et al., 2014; Suárez et al., 2014), but little is known about changes to striatal inputs arising from distinct brain regions, which may be differentially affected in PD.

MSNs require significant excitatory synaptic drive to spike (Wickens and Wilson, 1998), which they receive primarily from the cortex and thalamus (Kemp and Powell, 1971). Corticostriatal afferents have received the most attention in PD research, and dysregulation of synaptic plasticity at these inputs is thought to contribute to imbalanced basal ganglia circuit function (Kreitzer and Malenka, 2008; Surmeier et al., 2009). In contrast, fewer studies have examined the thalamostriatal system in PD (Smith et al., 2014). Here, we find that the relative strength of thalamic inputs to dMSNs and iMSNs is reversed after dopamine depletion, biasing excitatory drive to the indirect pathway. Consistent with this observation, chemogenetic and optogenetic inhibition of thalamostriatal terminals markedly improved parkinsonian motor deficits.

RESULTS

Reduced thalamostriatal drive to dMSNs in parkinsonian animals

To assay the relative excitatory input strength onto dMSNs versus iMSNs, we performed simultaneous voltage-clamp recordings from identified d/iMSN pairs in slices containing the dorsolateral striatum (DLS) from mice expressing Cre-dependent ChR2-EYFP in thalamostriatal (VGLUT2-Cre) or corticostriatal (Emx1-Cre) projections. One to two weeks before recordings, 6-hydroxydopamine (6OHDA) or saline was injected into the left medial forebrain bundle to produce parkinsonian or control animals, respectively (Figure 1D). In VGLUT2-Cre animals, strong EYFP expression was centered in Pf (Figure 1A), and dense axonal expression was observed in the DLS (Figure 1B). Brief light pulses through the microscope objective (Figure 1E) elicited fast excitatory postsynaptic currents (EPSCs) in both MSN subtypes (Figure 1F). On average, dMSNs in control animals displayed larger EPSC amplitudes than iMSNs (dMSN, 408.2 ± 86.0; iMSN, 311.1 ± 58.7 pA; n = 10; Figure 1G), and the average pairwise ratio revealed stronger dMSN synaptic drive (d:i ratio, 1.5 ± 0.3; Figure 1H). However, one to two weeks following 6OHDA-mediated ablation of striatal dopamine, EPSC amplitudes in iMSNs were significantly larger than those in dMSNs (dMSN, 180.0 ± 36.2; iMSN, 406.8 ± 80.9 pA; n = 16; Figure 1G), and the average pairwise ratio revealed a shift to preferential iMSN synaptic drive (d:i ratio, 0.70 ± 0.2; p = 0.016 vs. control; Figure 1H).

No relative change in corticostriatal synaptic strength in parkinsonian animals

ChR2-EYFP injections into Emx1-Cre animals resulted in extensive labeling of sensorimotor cortical neurons across layers (Figure 2A) and intense axonal labeling in the DLS (Figure 2B). As with thalamostriatal recordings, brief illumination (Figure 2E) elicited short-latency EPSCs in both MSN subtypes (Figure 2F). Paired recordings revealed larger EPSCs in dMSNs than iMSNs in control animals (dMSN, 403.6 ± 40.9; iMSN, 323.7 ± 45.2 pA; d:i ratio, 1.5 ± 0.2; n = 16; Figure 2G), as seen with our thalamostriatal stimulation and

in previous investigations of relative cortical drive to d/iMSN pairs (Kress et al., 2013). Recordings from 6OHDA-lesioned animals revealed no significant change in the relative corticostriatal drive to dMSNs and iMSNs compared to control animals (dMSN, 316.3 ± 43.3; iMSN, 240.8 ± 23.1 pA; d:i ratio, 1.4 ± 0.2; n = 12; p = 0.741 vs. control; Figure 2G,H).

Postsynaptic decrease in AMPAR-mediated responses at thalamo-dMSN synapses

The PD-associated reorganization of thalamostriatal excitatory drive might reflect changes in presynaptic glutamate release, which should be reflected in paired pulse ratio (PPR) measurements. By experimentally manipulating the external calcium concentration, we confirmed the sensitivity of optogenetically-evoked PPR measurements to changes in presynaptic release probability (Figure S1). After dopamine depletion, the d:iMSN PPR was unchanged at both corticostriatal (control vs. 6OHDA; 1.0 ± 0.1 vs. 1.0 ± 0.1, p = 0.899; n = 16 vs. 12; Figure 3A,B) and thalamostriatal (1.1 ± 0.1 vs. 1.0 ± 0.1, p = 0.755; n = 10 vs. 16) synapses (Figure 3C), suggesting no change in presynaptic release probability at thalamostriatal or corticostriatal synapses in parkinsonian animals. Furthermore, while studies in humans and other PD models have reported significant cell loss within CM/Pf, we saw no difference in the density of Pf cells between control and 6OHDA animals (Figure S2).

To test whether remodeling of thalamostriatal excitatory drive in parkinsonian animals was associated with alterations in postsynaptic function, we measured AMPA- and NMDA-EPSCs (Figure 3D). Thalamostriatal inputs showed a specific reduction in d:iMSN AMPA ratio, but not in d:iMSN NMDA ratio (control vs. 6OHDA; d:i AMPA, 1.2 ± 0.2 vs. 0.7 ± 0.1, p = 0.026; d:i NMDA, 1.1 ± 0.2 vs. 1.2 ± 0.3, p = 0.628; n = 18 vs. 15; Figure 3E). In theory, the decreased thalamostriatal d:iMSN AMPA ratio in parkinsonian mice could arise from a postsynaptic decrease in dMSN and/or an increase in iMSN EPSC amplitude. However, the AMPA:NMDA ratio was selectively decreased at thalamo-dMSN, but not thalamo-iMSN, synapses (control vs. 6OHDA AMPA:NMDA; dMSN, 4.3 ± 0.7 vs. 2.2 ± 0.3, n = 18 vs. 16, p = 0.015; iMSN, 4.3 ± 0.8 vs. 3.5 ± 0.5, n = 19 vs. 16, p = 0.389; Figure 3F), indicating a decrease in dMSN EPSC amplitude. Cortico-dMSN synapses showed a slight increase in AMPA:NMDA ratio (control vs. 6OHDA AMPA:NMDA; dMSN, 3.3 ± 0.3 vs. 4.5 ± 0.5, n = 16 vs. 13, p = 0.028; iMSN, 3.4 ± 0.5 vs. 3.8 ± 0.4, n = 12 vs. 12, p = 0.568; Figure 3F) but no significant change in d:iMSN AMPA and NMDA currents (control vs. 6OHDA; d:i AMPA, 1.4 ± 0.2 vs. 1.6 ± 0.2, p = 0.365; d:i NMDA, 1.3 ± 0.1 vs. 1.3 ± 0.2, p = 0.900; n = 10 vs. 10; Figure 3E).

Based on the specific decrease in thalamo-dMSN EPSCs after dopamine depletion, we next tested whether postsynaptic long-term depression (LTD) at this synapse is occluded in parkinsonian animals. Five minutes of 1 Hz thalamostriatal stimulation paired with postsynaptic dMSN depolarization to −40 mV produced a significant decrease in both EPSC amplitude and AMPA:NMDA ratio in control mice. However, no change in EPSC amplitude or AMPA:NMDA ratio was observed in parkinsonian mice (Figure 3G, H) (EPSC control vs. 6OHDA percent of baseline, 0.82 ± 0.07 vs. 1.00 ± 0.09, p = 0.04 vs. 0.48, n = 6 vs. 11; AMPA:NMDA control vs. 6OHDA percent of baseline, 0.79 ± 0.09 vs. 0.97 ± 0.05,

p = 0.03 vs. 0.28; baseline 6OHDA AMPA:NMDA as percent of control baseline, 0.53 ± 0.08, p = 0.02). Given that baseline AMPA:NMDA ratios were already significantly lower in parkinsonian mice vs. controls (Figure 3F), our data are consistent with the hypothesis that dopamine depletion induces an LTD-like loss of AMPA receptors at thalamo-dMSN synapses.

Inhibition of thalamostriatal inputs rescues parkinsonian motor behavior

Given the reported increase in firing of thalamic CM/Pf neurons in PD models (Jouve et al., 2010; Magnin et al., 2000; Orieux et al., 2000; Parr-Brownlie et al., 2009; Yan et al., 2008), and the decrease in thalamic connectivity with dMSNs after chronic dopamine depletion, we hypothesized that thalamostriatal inputs might be actively contributing to decreased spontaneous motor activity in parkinsonian mice through selective drive of the indirect pathway, relative to the direct pathway. We reasoned that disconnection of this pathway could rescue motor behavior. To test this hypothesis, we expressed hM4D, a Gi-coupled receptor activated exclusively by clozapine N-oxide (CNO) (Ferguson et al., 2011), in intralaminar thalamic neurons and implanted bilateral cannulae in DLS for local infusion of saline or CNO at thalamostriatal synapses (Figure 4A, Figure S4). The same animals received bilateral intra-DLS injections of saline or 6OHDA to produce bilateral, DLS-specific lesions of dopaminergic axons. In mice co-injected with ChR2 virus, optogenetically-evoked EPSCs in both dMSNs and iMSNs were strongly suppressed by bath application of CNO (baseline, 308.1 ± 97.0; CNO, 141.8 ± 65.7 pA; p = 0.025; n = 6; Figure S3), confirming hM4D-mediated suppression of glutamate release. Intra-DLS infusion and intraperitoneal (i.p.) injection of CNO into parkinsonian mice significantly increased the amount of time spent ambulating (saline vs. CNO: DLS, 33.8 ± 4.7% vs. 44.9 ± 6.5%, p = 0.039, n = 6; i.p., 37.3 ± 5.0% vs. 56.1 ± 5.2%, p = 0.003; n = 16), and i.p. injection decreased the amount of time spent freezing (DLS, 12.2 ± 4.8% vs. 7.1 ± 3.2%, p = 0.058; i.p., 19.8 ± 4.5% vs. 8.3 ± 2.1%, p = 0.012) relative to saline infusion/injection (Figure 4C). DLS infusion and i.p. injection of CNO also increased average center-point velocity (saline vs. CNO: DLS, 1.86 ± 0.23 vs. 2.59 ± 0.32 cm/s, p = 0.028; i.p., 2.0 ± 0.3 vs. 3.4 ± 0.5 cm/s, p = 0.009; Figure 4D). Activation of thalamic hM4D receptors in control animals had no effect on spontaneous motor behavior (saline vs. CNO: DLS, ambulation 37.1 ± 3.4% vs. 36.7 ± 4.2% p = 0.47, freezing 5.9 ± 1.4% vs. 4.7 ± 1.5% p = 0.22, velocity 2.0 ± 0.16 vs. 2.05 ± 0.21 cm/s, n = 8; i.p., ambulation 52.7 ± 3.5% vs. 53.5 ± 3.2% p = 0.888, freezing 4.1 ± 1.0% vs. 4.3 ± 1.4% p = 0.917, velocity 2.7 ± 0.2 vs. 2.8 ± 0.2 cm/s p = 0.660, n = 17; Figure 4C,D).

To test whether this amelioration of parkinsonian state is acute and reversible, we expressed the inhibitory light-gated proton pump eArch3.0 (Mattis et al., 2011) in intralaminar thalamic neurons and implanted bilateral optical fibers in DLS of animals injected bilaterally with saline or 6OHDA in DLS (Figure 4E, Figure S4). eArch3.0-mediated inactivation (10–15 mW/mm^2, 532nm, 30 s) of thalamostriatal terminals in parkinsonian animals rapidly and reversibly increased ambulation (pre 34.5 ± 10.8%, laser 58.9 ± 18.4%, post 35.3 ± 10.4%, p = 0.022, n = 6) decreased freezing (pre 100.8 ± 22.6%, laser 67.9 ± 18.1%, post 89.6 ± 16.6%, p = 0.009), and increased average center-point velocity (pre 0.69 ± 0.16, laser 1.01 ± 0.22, post 0.72 ± 0.15 cm/s, p = 0.008; Figure 4F–H). No changes were seen with eArch3.0-

mediated inhibition of thalamostriatal terminals in control animals (ambulation, pre 59.2 ± 12.2%, laser 56.2 ± 11.5%, post 54.9 ± 9.6%, p = 0.306; freezing, pre 62.2 ± 23.2%, laser 64.9 ± 25.8%, post 58.8 ± 22.3%, p = 0.366; velocity, pre 1.08 ± 0.18, laser 1.03 ± 0.18, post 1.02 ± 0.15 cm/s, p = 0.227, n = 9; Figure 4G,H), consistent with a detrimental gain-of-function of thalamostriatal inputs in parkinsonian animals.

DISCUSSION

Historically, cortical and thalamic terminals have been differentiated by their expression of VGLUT1 and VGLUT2, respectively (Fremeau et al., 2001; Fujiyama et al., 2001; Herzog et al., 2001). Recent evidence suggests there is a selective loss of striatal VGLUT2+ terminals in monkey MPTP models (Villalba et al., 2013). Our data indicate that reduced thalamostriatal synaptic input is specific to dMSNs in parkinsonian animals. Although our study did not selectively target Pf, other work has found distinct synaptic properties at Pf vs. central lateral thalamic inputs (Ellender et al., 2013), indicating that it will be critical to learn whether changes to thalamostriatal inputs in parkinsonian animals apply only to specific intralaminar nuclei or more broadly.

Neurons in the intralaminar thalamus have been previously implicated in PD. CM/Pf neurons in PD patients and animal models show higher firing rates and increased oscillatory activity (Jouve et al., 2010; Orieux et al., 2000; Parr-Brownlie et al., 2009; Yan et al., 2008). In parkinsonian rats, Pf lesions decrease response latency on a motivational task (Henderson et al., 2005), and Pf DBS rescues sensorimotor neglect (Jouve et al., 2010). In PD patients, Pf DBS effectively reduces tremor and, as seen in rodent models, reduces levodopa-induced dyskinesia (Caparros-Lefebvre et al., 1999; Mazzone et al., 2006; Peppe et al., 2008; Stefani et al., 2009). These studies, together with our data, support the notion that a parkinsonian gain-of-function of intralaminar thalamus contributes to basal ganglia pathophysiology in PD (Chen et al., 2014). Indeed, CM/Pf inactivation using hM4D or eArch3.0 showed no effect in control animals, consistent with previous studies that found no effect of CM/Pf lesion on spontaneous motor behavior (Henderson et al., 2005; Quiroz-Padilla et al., 2006). Thus, the normal role of CM/Pf may be in sensory-driven rather than internally-driven behavior (Matsumoto et al., 2001; Minamimoto et al., 2005).

The lack of change in the relative d/iMSN cortical synaptic drive in our study is quite surprising given the rich literature surrounding corticostriatal synaptic reorganization in PD, for example the loss of VGLUT1-associated spines in parkinsonian mice and their aberrant restoration in L-DOPA-induced dyskinesia (Zhang et al., 2013). However, even with significant alterations to dMSN and iMSN morphology and physiology, broad activation of Thy1-ChR2 afferents in striatum reveals minor changes in overall EPSC amplitudes (Fieblinger et al., 2014). Our data suggest that, despite the many changes seen to the presumptive corticostriatal anatomy in PD models, the ultimate outcome of these changes is the maintenance of relative drive to the direct and indirect pathways.

Significant CM/Pf cell loss occurs in PD patients and monkey MPTP models. However, we did not see evidence for Pf cell death in our 6-OHDA model. It is therefore difficult to predict whether the changes seen here are recapitulated in patients and primate models.

Future studies should investigate this issue as the pathway-specific reorganization seen here would deleteriously add to the known thalamostriatal changes in PD discussed above. Overall, our results highlight the need for a better understanding of the molecular mechanisms behind thalamostriatal plasticity in normal and disease states, and closer consideration of the thalamus as a major player in the pathophysiology of Parkinson's disease.

EXPERIMENTAL PROCEDURES

All experiments were approved by the Institutional Animal Care and Use Committee at the University of California, San Francisco.

Surgeries

6–10-week-old mice were anesthetized and placed in a stereotaxic frame, and a 33-gauge needle (Plastics One) was inserted for viral injections into cortex (AP +0.5/1.5, ML +/−2.0, DV −1.0 from dura) or thalamus (AP −2.3, ML +/−0.5, DV −3.25 from dura). A volume of 0.75 μl/site of virus was injected at a rate of 0.2 μl/min. Two weeks later, the scalp was reopened and 1 μl of 5 μg/μl 6-hydroxydopamine (6OHDA; Sigma-Aldrich) was injected unilaterally into the medial forebrain bundle (MFB; AP −1.0, ML −1.0, DV −4.9 from dura) or bilaterally into the DLS (AP +0.8, ML +/− 2.2, DV −2.5 from dura).

Electrophysiology

1–2 weeks after 6-OHDA/saline injection, acute slices (300 μm) were cut through the DLS in sucrose-based artificial cerebrospinal fluid (ACSF). Simultaneous voltage-clamp recordings were made from one D1-Tomato+ and one D1-Tomato− MSN using 2–4 MΩ glass electrodes. Light pulses (470 nm, 0–2 mW/mm^2, 0.5–5 ms duration) were delivered through a 40x immersion objective at 0.15 Hz using a high-intensity LED (Thorlabs LED4C driven by a Prizmatix BLCC-2).

Open Field Behavior

1–2 weeks after 6-OHDA/saline injection, activity in the open field was tracked using ETHOVISION 9 software (Noldus). Statistical significance was evaluated using a two-way ANOVA and post-hoc Bonferroni-corrected paired student's t-test. Animals were excluded if incomplete bilateral loss of TH+ axonal labeling in DLS was achieved (6OHDA group), quantified as <30% loss of total striatal TH staining, or if the location of the cannula/fiber tip was outside of DLS (both groups).

Histology

Mice were transcardially perfused with PBS followed by 4% paraformaldehyde (PFA), brains were rapidly dissected out and placed into 4% PFA overnight. Brains were rinsed in PBS, cryoprotected, and sliced (30 μm). After blocking and permeabilization, slices were incubated in primary antibody (rabbit anti-tyrosine hydroxylase 1:500, Pel-Freeze; mouse anti-RFP 1:500, Rockland Immunochemicals; rabbit anti-cerebellin 1, 1:250, Abcam) overnight at 4°C. Slices were then incubated in secondary antibody (donkey anti-mouse

Alexa568, donkey anti-rabbit Alexa647, 1:1000, Invitrogen) for 1 h at room temperature and mounted onto slides for imaging.

Supplementary Material

Refer to Web version on PubMed Central for supplementary material.

Acknowledgments

We thank D. Schulte, A.M. Lee, and members of the Kreitzer Lab for helpful advice on experiments, comments on the manuscript, and technical assistance. This research was supported by NIH National Research Service Award 1F31NS080543 (P.R.L.P.), the Swiss National Science Foundation (A.L.L), and NIH R01 NS064984 (A.C.K.).

References

Albin RL, Young AB, Penney JB. The functional anatomy of basal ganglia disorders. Trends Neurosci. 1989; 12:366–375.10.1016/0166-2236(89)90074-X [PubMed: 2479133]

Caparros-Lefebvre D, Blond S, Feltin MP, Pollak P, Benabid AL. Improvement of levodopa induced dyskinesias by thalamic deep brain stimulation is related to slight variation in electrode placement: possible involvement of the centre median and parafascicularis complex. J Neurol Neurosurg Psychiatry. 1999; 67:308–314.10.1136/jnnp.67.3.308 [PubMed: 10449551]

Chen CH, Fremont R, Arteaga-Bracho EE, Khodakhah K. Short latency cerebellar modulation of the basal ganglia. Nat Neurosci. 2014; 17:1767–1775.10.1038/nn.3868 [PubMed: 25402853]

Day M, Wang Z, Ding J, An X, Ingham CA, Shering AF, Wokosin D, Ilijic E, Sun Z, Sampson AR, Mugnaini E, Deutch AY, Sesack SR, Arbuthnott GW, Surmeier DJ. Selective elimination of glutamatergic synapses on striatopallidal neurons in Parkinson disease models. Nat Neurosci. 2006; 9:251–259. [PubMed: 16415865]

DeLong MR. Primate models of movement disorders of basal ganglia origin. Trends Neurosci. 1990; 13:281–285.10.1016/0166-2236(90)90110-V [PubMed: 1695404]

Ehringer H, Hornykiewicz O. Verteilung Von Noradrenalin Und Dopamin (3-Hydroxytyramin) Im Gehirn Des Menschen Und Ihr Verhalten Bei Erkrankungen Des Extrapyramidalen Systems. Klin Wochenschr. 1960; 38:1236–1239.10.1007/BF01485901 [PubMed: 13726012]

Ellender TJ, Harwood J, Kosillo P, Capogna M, Bolam JP. Heterogeneous properties of central lateral and parafascicular thalamic synapses in the striatum. J Physiol. 2013; 591:257–72.10.1113/jphysiol.2012.245233 [PubMed: 23109111]

Ferguson SM, Eskenazi D, Ishikawa M, Wanat MJ, Phillips PEM, Dong Y, Roth BL, Neumaier JF. Transient neuronal inhibition reveals opposing roles of indirect and direct pathways in sensitization. Nat Neurosci. 2011; 14:22–24.10.1038/nn.2703 [PubMed: 21131952]

Fieblinger T, Graves SM, Sebel LE, Alcacer C, Plotkin JL, Gertler TS, Chan CS, Heiman M, Greengard P, Cenci MA, Surmeier DJ. Cell type-specific plasticity of striatal projection neurons in parkinsonism and L-DOPA-induced dyskinesia. Nat Commun. 2014; 5:1–15.10.1038/ncomms6316

Fremeau RT, Troyer MD, Pahner I, Nygaard GO, Tran CH, Reimer RJ, Bellocchio EE, Fortin D, Storm-Mathisen J, Edwards RH. The expression of vesicular glutamate transporters defines two classes of excitatory synapse. Neuron. 2001; 31:247–260.10.1016/S0896-6273(01)00344-0 [PubMed: 11502256]

Fujiyama F, Furuta T, Kaneko T. Immunocytochemical localization of candidates for vesicular glutamate transporters in the rat cerebral cortex. J Comp Neurol. 2001; 435:379–387. [PubMed: 11406819]

Henderson JM, Schleimer SB, Allbutt H, Dabholkar V, Abela D, Jovic J, Quinlivan M. Behavioural effects of parafascicular thalamic lesions in an animal model of parkinsonism. Behav Brain Res. 2005; 162:222–232.10.1016/j.bbr.2005.03.017 [PubMed: 15970217]

Herzog E, Bellenchi GC, Gras C, Bernard V, Ravassard P, Bedet C, Gasnier B, Giros B, El Mestikawy S. The existence of a second vesicular glutamate transporter specifies subpopulations of glutamatergic neurons. J Neurosci. 2001; 21:RC181. 20015807 [pii]. [PubMed: 11698619]

Jouve L, Salin P, Melon C, Kerkerian-Le Goff L. Deep brain stimulation of the center median-parafascicular complex of the thalamus has efficient anti-parkinsonian action associated with widespread cellular responses in the basal ganglia network in a rat model of Parkinson's disease. J Neurosci. 2010; 30:9919–9928.10.1523/JNEUROSCI.1404-10.2010 [PubMed: 20660274]

Kemp JM, Powell TP. The termination of fibres from the cerebral cortex and thalamus upon dendritic spines in the caudate nucleus: a study with the Golgi method. Philos Trans R Soc Lond B Biol Sci. 1971; 262:429–439.10.1098/rstb.1971.0105 [PubMed: 4107496]

Kreitzer AC, Malenka RC. Striatal Plasticity and Basal Ganglia Circuit Function. Neuron. 200810.1016/j.neuron.2008.11.005

Kress GJ, Yamawaki N, Wokosin DL, Wickersham IR, Shepherd GMG, Surmeier DJ. Convergent cortical innervation of striatal projection neurons. Nat Neurosci. 2013; 16:665–7.10.1038/nn.3397 [PubMed: 23666180]

Magnin M, Morel A, Jeanmonod D. Single-unit analysis of the pallidum, thalamus and subthalamic nucleus in parkinsonian patients. Neuroscience. 2000; 96:549–564.10.1016/S0306-4522(99)00583-7 [PubMed: 10717435]

Matsumoto N, Minamimoto T, Graybiel AM, Kimura M. Neurons in the thalamic CM-Pf complex supply striatal neurons with information about behaviorally significant sensory events. J Neurophysiol. 2001; 85:960–976. [PubMed: 11160526]

Mattis J, Tye KM, Ferenczi Ea, Ramakrishnan C, O'Shea DJ, Prakash R, Gunaydin La, Hyun M, Fenno LE, Gradinaru V, Yizhar O, Deisseroth K. Principles for applying optogenetic tools derived from direct comparative analysis of microbial opsins. Nat Methods. 2011; 9:159–172.10.1038/nmeth.1808 [PubMed: 22179551]

Mazzone P, Stocchi F, Galati S, Insola A, Altibrandi MG, Modugno N, Tropepi D, Brusa L, Stefani A. Bilateral implantation of centromedian-parafascicularis complex and GPi: A new combination of unconventional targets for deep brain stimulation in severe Parkinson disease. Neuromodulation. 2006; 9:221–228.10.1111/j.1525-1403.2006.00063.x [PubMed: 22151710]

Minamimoto T, Hori Y, Kimura M. Complementary process to response bias in the centromedian nucleus of the thalamus. Science. 2005; 308:1798–1801.10.1126/science.1109154 [PubMed: 15961671]

Orieux G, Francois C, Féger J, Yelnik J, Vila M, Ruberg M, Agid Y, Hirsch EC. Metabolic activity of excitatory parafascicular and pedunculopontine inputs to the subthalamic nucleus in a rat model of Parkinson's disease. Neuroscience. 2000; 97:79–88.10.1016/S0306-4522(00)00011-7 [PubMed: 10771341]

Parr-Brownlie LC, Poloskey SL, Bergstrom DA, Walters JR. Parafascicular thalamic nucleus activity in a rat model of Parkinson's disease. Exp Neurol. 2009; 217:269–281.10.1016/j.expneurol.2009.02.010 [PubMed: 19268664]

Peppe A, Gasbarra A, Stefani A, Chiavalon C, Pierantozzi M, Fermi E, Stanzione P, Caltagirone C, Mazzone P. Deep brain stimulation of CM/PF of thalamus could be the new elective target for tremor in advanced Parkinson's Disease? Park Relat Disord. 2008; 14:501–504.10.1016/j.parkreldis.2007.11.005

Quiroz-Padilla MF, Guillazo-Blanch G, Vale-Martínez A, Martí-Nicolovius M. Excitotoxic lesions of the parafascicular nucleus produce deficits in a socially transmitted food preference. Neurobiol Learn Mem. 2006; 86:256–263.10.1016/j.nlm.2006.03.007 [PubMed: 16714125]

Smith Y, Galvan A, Ellender TJ, Doig N, Villalba RM, Huerta-Ocampo I, Wichmann T, Bolam JP. The thalamostriatal system in normal and diseased states. Front Syst Neurosci. 2014; 8:5.10.3389/fnsys.2014.00005 [PubMed: 24523677]

Stefani A, Peppe A, Pierantozzi M, Galati S, Moschella V, Stanzione P, Mazzone P. Multi-target strategy for Parkinsonian patients: The role of deep brain stimulation in the centromedian-parafascicularis complex. Brain Res Bull. 2009; 78:113–118.10.1016/j.brainresbull.2008.08.007 [PubMed: 18812214]

Suárez LM, Solís O, Caramés JM, Taravini IR, Solís JM, Murer MG, Moratalla R. L-DOPA treatment selectively restores spine density in dopamine receptor d2-expressing projection neurons in dyskinetic mice. Biol Psychiatry. 2014; 75:711–722.10.1016/j.biopsych.2013.05.006 [PubMed: 23769604]

Surmeier DJ, Plotkin J, Shen W. Dopamine and synaptic plasticity in dorsal striatal circuits controlling action selection. Curr Opin Neurobiol. 200910.1016/j.conb.2009.10.003

Villalba, RM.; Wichmann, T.; Smith, Y. Neuroscience 2013 Abstracts. Vol. 2013. San Diego, CA: Society for Neuroscience; 2013. Preferential loss of thalamostriatal over corticostriatal glutamatergic synapses in parkinsonian monkeys. 240.02. Online

Wickens JR, Wilson CJ. Regulation of action-potential firing in spiny neurons of the rat neostriatum in vivo. J Neurophysiol. 1998; 79:2358–2364. [PubMed: 9582211]

Yan W, Zhang QJ, Liu J, Wang T, Wang S, Liu X, Chen L, Gui ZH. The neuronal activity of thalamic parafascicular nucleus is conversely regulated by nigrostriatal pathway and pedunculopontine nucleus in the rat. Brain Res. 2008; 1240:204–212.10.1016/j.brainres.2008.09.015 [PubMed: 18823953]

Zhang Y, Meredith GE, Mendoza-Elias N, Rademacher DJ, Tseng KY, Steece-Collier K. Aberrant restoration of spines and their synapses in L-DOPA-induced dyskinesia: involvement of corticostriatal but not thalamostriatal synapses. J Neurosci. 2013; 33:11655–67.10.1523/JNEUROSCI.0288-13.2013 [PubMed: 23843533]

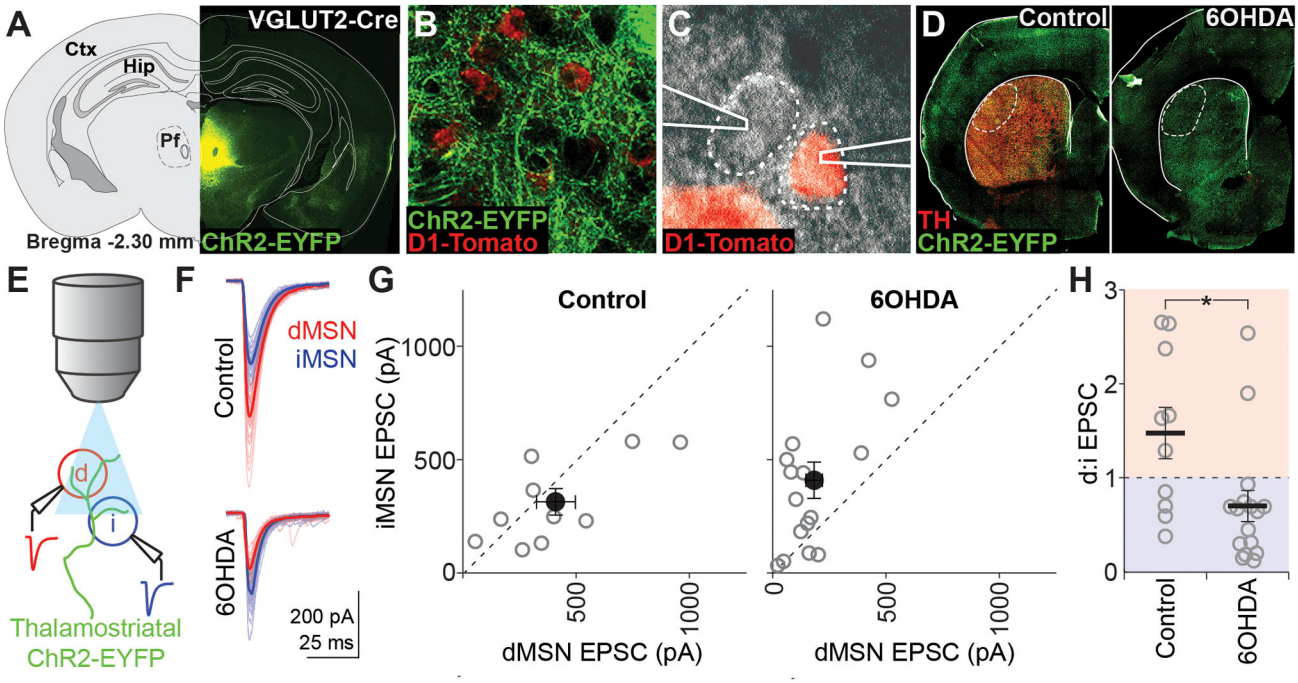

Figure 1. Dopamine depletion selectively reduces thalamic input to dMSNs

(A) AAV-DIO-ChR2-EYFP expression targeting intralaminar thalamus in VGLUT2-cre x D1-Tomato mice. Ctx, cortex; Hip, hippocampus; Pf, parafascicular nucleus.

(B) ChR2-EYFP+ axons in the DLS surrounding D1-Tomato+ dMSNs.

(C) DIC image of simultaneous patch-clamp recordings from one D1-Tomato+ and one D1-Tomato− MSN.

(D) Epifluorescence image of ChR2-EYFP and tyrosine hydroxylase (TH) expression in coronal sections containing the DLS of saline- (control) and 6OHDA-injected animals. Recordings were obtained within the dotted region.

(E) Schematic of recording setup: whole-cell responses to thalamostriatal stimulation evoked by 470nm LED pulses through the objective were recorded simultaneously from one dMSN (red) and one iMSN (blue).

(F) Example traces from a pair of MSNs in a control and 6OHDA-lesioned animal. Thick traces are averages and thin traces are individual sweeps.

(G) Individual (grey) and mean (black) values for dMSN and iMSN EPSC amplitudes for all recorded pairs in control (left, n=10 pairs) and 6OHDA-lesioned (right, n=16 pairs) animals.

(H) Pairwise ratios of dMSN and iMSN EPSC amplitudes in control and 6OHDA-lesioned animals. Points above 1 (red shading) represent dMSN-favored pairs and points below 1 (blue shading) represent iMSN-favored pairs. All summary data are mean ± SEM. Asterisk is p=0.016.

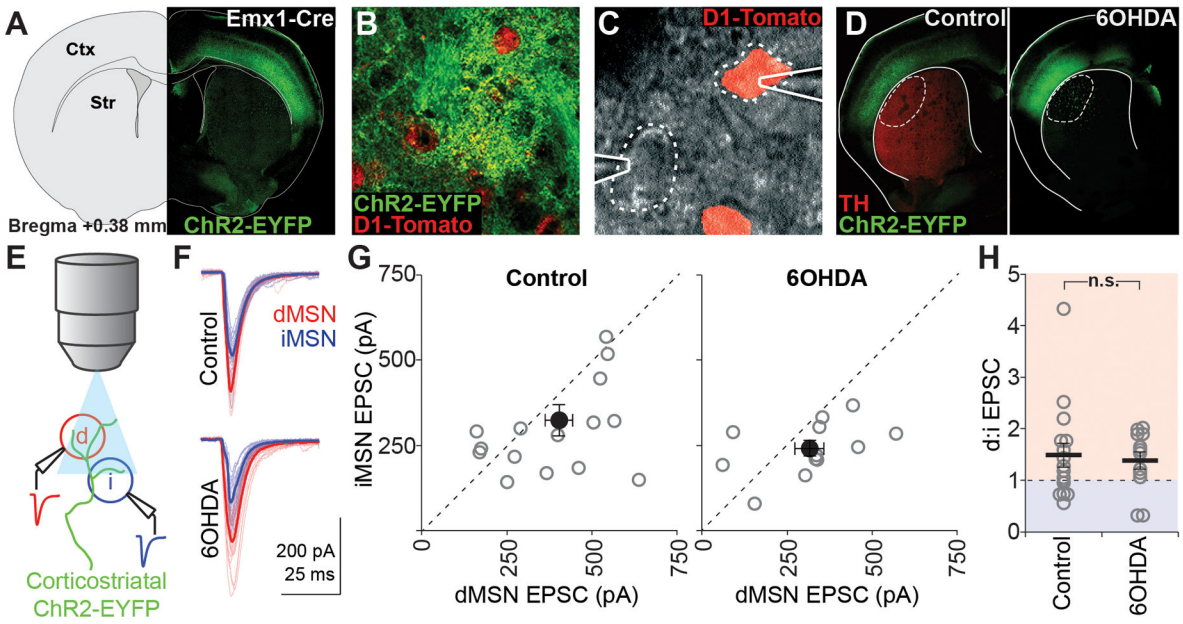

Figure 2. Maintenance of relative corticostriatal drive after dopamine depletion

(A) AAV-DIO-ChR2-EYFP expression targeting sensorimotor cortex in Emx1-cre x D1-Tomato mice. Ctx, cortex; Str, striatum.

(B) ChR2-EYFP+ axons in the DLS surrounding D1-Tomato+ dMSNs.

(C) DIC image of simultaneous patch-clamp recordings from one D1-Tomato+ and one D1-Tomato− MSN.

(D) Epifluorescence image of ChR2-EYFP and tyrosine hydroxylase (TH) expression in coronal sections containing the DLS of saline- (control) and 6OHDA-injected animals. Recordings were obtained within the dotted region.

(E) Schematic of recording setup: whole-cell responses to corticostriatal stimulation evoked by 470nm LED pulses through the objective were recorded simultaneously from one dMSN (red) and one iMSN (blue).

(F) Example traces from a pair of MSNs in a control and a 6OHDA-lesioned animal. Thick traces are averages and thin traces are individual sweeps.

(G) Individual (grey) and mean (black) values for dMSN and iMSN EPSC amplitudes for all recorded pairs in control (left, n=16 pairs) and 6OHDA-lesioned (right, n=12 pairs) animals.

(H) Pairwise ratios of dMSN and iMSN EPSC amplitudes in control and 6OHDA-lesioned animals. All summary data are mean ± SEM; n.s. is not significant.

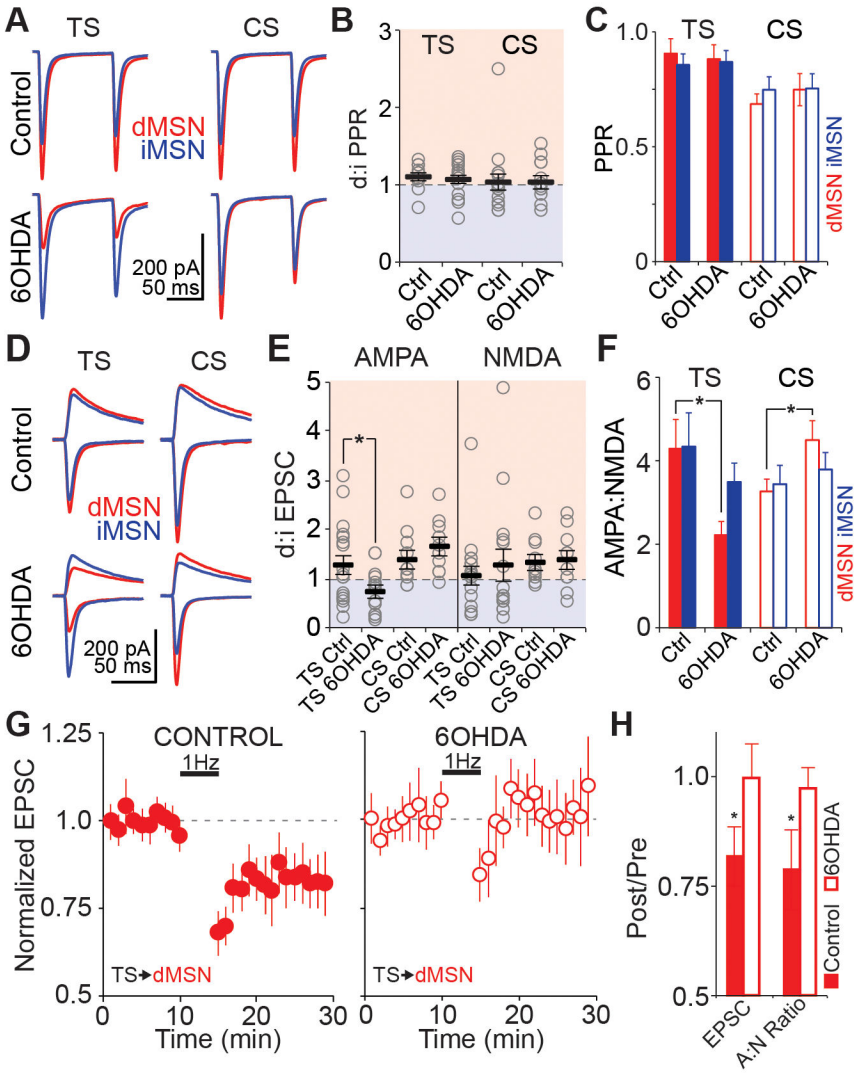

Figure 3. Selective reduction in postsynaptic AMPAR-mediated currents at thalamo-dMSN synapses in parkinsonian animals

(A) Averaged traces from all dMSN (red) and iMSN (blue) pairs showing thalamostriatal (TS) and corticostriatal (CS) responses in control and 6OHDA-lesioned animals. For each individual pair, the paired pulse ratio (PPR) was calculated as EPSC2/EPSC1.

(B) d:iMSN ratio of PPR at TS (left) and CS (right) synapses. Gray circles are individual pairs, black bars are group means. TS control n=10, TS 6OHDA n=16, CS control n=16, CS 6OHDA n=12.

(C) Unpaired data showing average PPR at TS (filled bars) and CS (open bars) synapses for dMSNs and iMSNs in control (Ctrl) and 6OHDA-lesioned animals. All summary data are presented as mean ± SEM. TS control n=10, TS 6OHDA n=16, CS control n=16, CS 6OHDA n=12.

(D) Averaged traces from all dMSN (red) and iMSN (blue) pairs showing TS and CS responses in control and 6OHDA-lesioned animals. For each pair, lower traces were

recorded at −80 mV (AMPA) and upper traces were recorded at +40 mV (NMDA, calculated 50 ms post-stimulus).

(E) d:iMSN ratio of AMPA (left) and NMDA (right) currents at TS and CS synapses. Gray circles are individual pairs, black bars are group means. TS control n=18, TS 6OHDA n=15, CS control n=10, CS 6OHDA n=10. Asterisk is p=0.026.

(F) Unpaired data showing average values of AMPA:NMDA ratios at TS (filled bars) and CS (open bars) synapses for dMSNs and iMSNs in control (Ctrl) and 6OHDA-lesioned animals. TS control n=18, TS 6OHDA n=16, CS control n=13, CS 6OHDA n=12. Asterisk is p=0.015.

(G) Baseline-normalized EPSC amplitudes before and after 5 min of 1 Hz stimulation of TS inputs to dMSNs paired with postsynaptic depolarization to −40 mV in slices from control (left, n=6) and 6OHDA-lesioned (right, n=11) animals.

(H) Change in EPSC amplitude and AMPA/NMDA ratio relative to baseline after 1 Hz induction protocol. Control n=6, 6OHDA n=11. Asterisks are p=0.043 (EPSC) and p=0.034 (AMPA/NMDA).

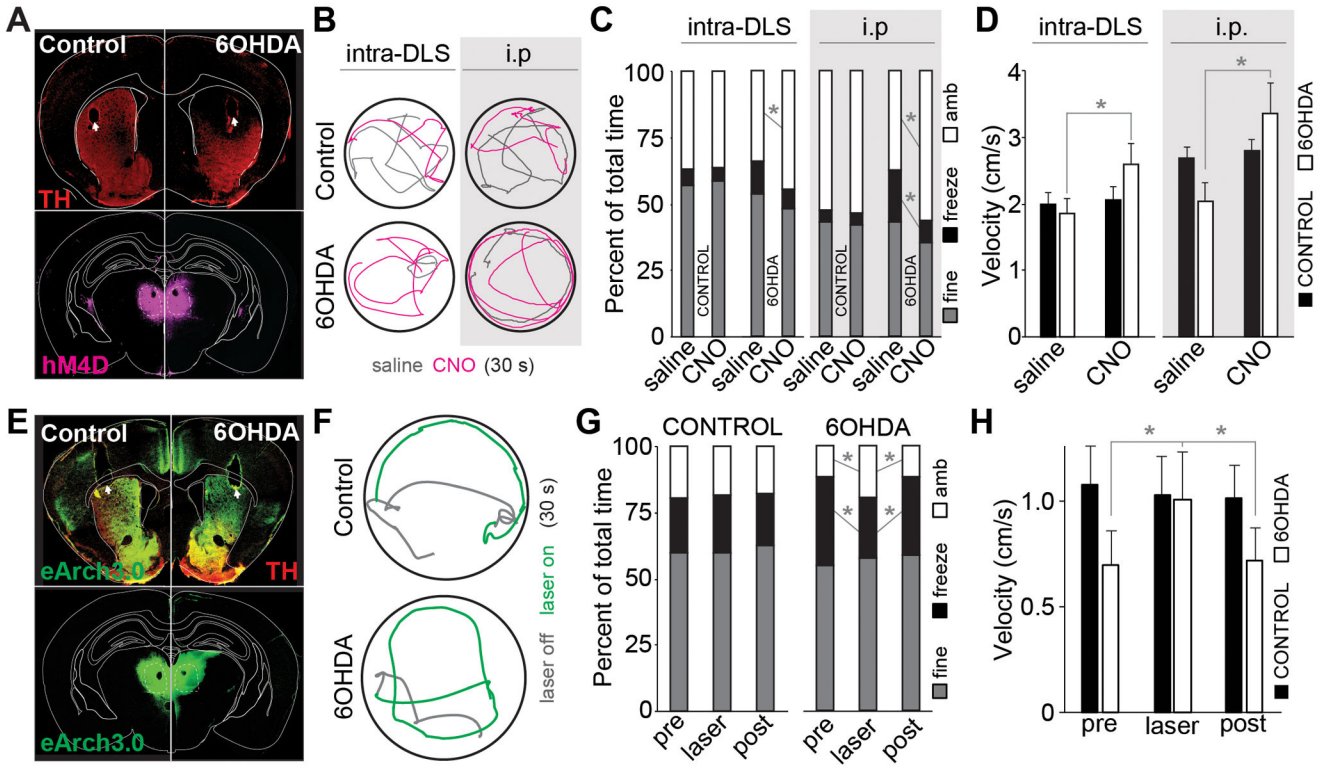

Figure 4. hM4D- and eArch3.0-mediated inhibition of thalamostriatal inputs rescues parkinsonian motor behavior

(A) Bilateral dorsolateral striatal 6ODHA lesions and cannula implants (top) and thalamic hM4D-mCherry expression (bottom) in example control (left) and 6OHDA-lesioned (right) animals. Arrows indicate cannula tracts, dotted line indicates parafascicular nucleus.

(B) Example center-point trajectories of control (top) and 6OHDA-lesioned (bottom) mice given saline (grey) or CNO (magenta) by infusion into dorsolateral striatum (intra-DLS, left) or i.p. injection (i.p., right). Each trace represents 30 s of behavior.

(C) Average percent of time spent freezing, ambulating, or engaged in fine movement during a 15-minute open field session for control and 6OHDA-lesioned animals infused into the DLS (left) or injected i.p. (right) with saline or CNO. Control: DLS n=8, i.p. n=17; 6OHDA: DLS n=6, i.p. n=16. DLS: asterisk is ambulation p=0.039; i.p. asterisks are p=0.0124 for freezing, p=0.003 for ambulation.

(D) Average total velocity for DLS infusions (left) and i.p. injections (right) of saline and CNO in control and 6OHDA-lesioned animals. Asterisks are p=0.028 for DLS and p=0.009 for i.p.

(E) Bilateral dorsolateral striatal 6OHDA lesions and optic fiber implants in the DLS (top) of animals expressing eArch3.0 in thalamus (bottom). Arrows indicate fiber tracts, dotted line indicates parafascicular nucleus.

(F) Example trajectories of a control and a 6OHDA-lesioned mouse before (grey) or after (green) laser onset. Each trace represents 30 s of behavior.

(G) Average percent of time spent freezing, ambulating, or engaged in fine movement across a 15-minute open field session for control and 6OHDA-lesioned animals before, during, and after 560 nm laser stimulation of eArch3.0-expressing thalamostriatal terminals. Control

n=9, 6OHDA n=6. Asterisk are ambulation pre vs. laser p=0.022, freezing pre vs. laser p=0.009, ambulation laser vs post p=0.020, freezing laser vs. post p=0.001.
(H) Average total velocity before, during, and after eArch3.0-mediated inhibition of thalamostriatal terminals in the DLS of control and 6OHDA-lesioned animals. Asterisks are p=0.008 for pre vs. laser and p=0.007 for laser vs. post.